

Probing the Enzyme Catalytic Mechanism by Nuclear Magnetic Resonance - A Case Study of a Serine Protease

Sergiy I. Tyukhtenko^a, Yao-Te Huang^a (黃耀德), Ta-hsin Lin^{a,c} (林達顯),
Chinpan Chen^a (陳金榜), Chi-Fon Chang^a (張七鳳), Shin-Jye Lee^a (李欣潔),
Alexandra V. Litvinchuk^a, Jei-Fu Shaw^b (蕭介夫),
Yen-Chywan Liaw^c (廖彥銓) and Tai-huang Huang^{a,d,*} (黃太煌)

^a*Institute of Biomedical Sciences, ^bInstitute of Botany and ^cInstitute of Molecular Biology, Academia Sinica, Nankang, Taipei, Taiwan 11529, R.O.C.*

^d*Department of Physics, National Taiwan Normal University, Taipei, Taiwan, R.O.C.*

^e*Department of Medical Research and Education, Veterans General Hospital, and Institute of Biochemistry, National Yang-Ming University, Peitou, Taipei, Taiwan, R.O.C.*

Serine proteases are among the most studied enzymes for their role as model enzymes for studying the enzyme catalytic mechanism and medical interest in their inhibition. We have applied NMR methods to determine the structure, dynamics, and catalytic mechanism of a serine protease, *E. coli* thioesterase/protease I (TEP-I). In this article we review the results of our efforts. We showed that TEP-I is an α/α type SNGH-hydrolase with Ser¹⁰, Asp¹⁵⁴ and His¹⁵⁷ as the catalytic triad residues. In free TEP-I, His¹⁵⁷ was found to form a strong hydrogen bond to Asp¹⁵⁴, but not to Ser¹⁰-O H. Model-free analysis of ¹⁵N-T₁, ¹⁵N-T₂ and ¹H-¹⁵N NOE data revealed that TEP-I is a rigid protein with a flexible catalytic binding pocket. Slow motion involving segments around the catalytic site was detected. The formation of Michaelis complex (MC) between TEP-I and a transition state analogue, diethyl p-nitrophenyl phosphate (DENP), and its subsequent conversion to the tetrahedral complex (TC) follow a two-step process, a fast formation of MC followed by a slow conversion to TC. In both steps residues perturbed were confined mainly to four conserved segments comprising the active site. Comparable magnitudes of chemical shift perturbations were detected in both steps. From the large chemical shift perturbation upon conversion from MC to TC we proposed that the amide protons of Ser¹⁰ and Gly⁴⁴ serve as the oxyanion-hole proton donors to stabilize the tetrahedral adduct. The pattern of residues perturbed in both steps suggests a sequential, stepwise structural change upon binding of DENP.

Keywords: Enzyme catalysis; NMR; Protein structure; Thioesterase; Serine protease.

INTRODUCTION

Enzymes enhance the rate of chemical reactions by many orders of magnitudes.¹⁻⁷ How they work is a basic, as well as practical question, which has intrigued scientists for centuries. Significant progress has been made but the question is still far from fully understood. Serine proteases are among the most studied enzymes for their roles as model enzymes for studying the mechanism of enzyme catalysis and medical interest in their inhibition. This class of enzymes uses a "catalytic triad" of serine, histidine, and aspartic acid as the catalytic residues. The general catalytic sequence of serine proteases includes formation of a non-covalent Michaelis complex. Nucleophilic attack by the active site Ser

residue of the peptide carbonyl group results in the formation of a tetrahedral oxyanion intermediate, which subsequently releases the C-terminal product fragment to form the acyl-enzyme at the Ser residue. In the second deacylation reaction, hydrolytic attack by a water molecule on the ester carbonyl group leads to the formation of the second tetrahedral intermediate, which collapses to give the N-terminal product fragment and the restoration of free enzyme. Formation of multiple intermediates with lower activation energy than the overall uncatalyzed step constitutes the main theme of the transition state theory for enzyme catalysis.²⁻⁶ Therefore, in order to understand the mechanism of enzyme catalysis, it is necessary to determine the structure and understand the source of the binding power of the enzyme for all intermediate states.

Dedicated to Professor Sunney I. Chan on the occasion of his 67th birthday and his retirement from professional life.

* Corresponding author. Tel: +886-2-2652-3036; fax: 2-2788-7641; e-mail: bmthh@ibms.sinica.edu.tw

However, the lifetimes of transition states are very short (about 10^{-13} s) and are very hard to characterize. In 1969, Wolfenden recognized that transition state analogues (TSA), molecules that mimic the transition state of an enzyme-catalyzed reaction, should bind tightly to the enzyme and could be used as a model of the transition state.⁸ Use of TSAs has provided considerable insight into the interactions between TSA and the enzyme and the structures of the intermediate species.⁹

E. coli thioesterase/protease I (TEP-I) is a 182-amino-acid single peptide protein.¹⁰⁻¹² It has been classified as a member of a new subclass of the lipolytic enzymes with diverse substrate specificity and regiospecificity.^{13,14} TEP-I catalyzes the hydrolytic cleavage of long chain (C_{12} - C_{18}) fatty acyl-coenzyme A (CoA) thioesters *in vitro* and also cleaves fatty-acyl carrier protein (ACP) thioesters at a rate of 10^3 to 10^4 times slower than acyl-coA esters of the same length.^{15,16} Thus, it terminates fatty acid chain growth during fatty acid synthesis by hydrolysis of the acyl thioester linkage between the fatty acid and phosphopantetheine cofactor of fatty acid synthesis. This protein has also been shown to possess arylesterase activity.¹³ Cho and Cronan further showed that the same active site is used for both fatty acid and amino acid substrates and that it behaves as a thioesterase *in vivo*.¹⁷ Defects in the export of this enzyme result in disrupted regulation of fatty acid synthesis.¹⁸ The exact physiological role of the protein is unclear as the deletion of this gene does not seem to produce any change in growth phenotype.^{11,12} The rather versatile enzymatic activities of *E. coli* thioesterase/protease I render it a good candidate for further engineering for industrial applications.

A team of four laboratories in Academia Sinica have been investigating the structure, dynamics, and enzyme catalytic mechanism of TEP-I.¹⁹⁻²² In this article we review the results of our efforts in characterizing the molecular events of the catalytic process of *E. coli* thioesterase/protease I using heteronuclear multidimensional NMR techniques.¹⁹⁻²²

RESULTS AND DISCUSSION

Structure of TEP-I¹⁹

TEP-I is a well-behaved protein with excellent pH and temperature stabilities and NMR chemical shift dispersion. Complete resonance assignment of this 182 amino acid protein was achieved through analysis of a large set of heteronuclear multi-dimensional NMR data of uniformly and specifically amino acid $^{13}C/^{15}N$ -labeled protein samples.¹⁹ The

secondary structure topology of TEP-I were established from a number of NMR-determined parameters, including chemical shift indices,²³⁻²⁵ the magnitude of NH-C α H coupling constants, and the patterns of short- and medium-range NOEs.²⁶ The secondary structural topology of *E. coli* thioesterase I was found to be composed of seven α -helices and four strands, similar to the core structure of common lipases. The tertiary fold is further determined by both NMR (Huang, unpublished results) and X-ray crystallography,²⁷ and a ribbon representation of the X-ray structure is shown in Fig. 1. The tertiary folding is of the α/α type. The structural features fit well to the new SGNH-hydrolase family.²⁸ Ser¹⁰, Asp¹⁵⁴ and His¹⁵⁷ were positioned in a linear fashion, and they were identified as the catalytic triad residues (PDB code 1JRL), thus, classifying TEP-I as a serine protease. The amide protons of Ser¹⁰ and Gly⁴⁴, and the side chain amino protons of Asn⁷³ were proposed to be the oxyanion hole donors. These assignments were confirmed by our NMR results, as described below.

Dynamics of TEP-I²⁰

NMR is a powerful technique for probing the dynamics of proteins in atomic detail from analyzing the relaxation rates of each nucleus. The relaxation data, including ^{15}N -R $_1$

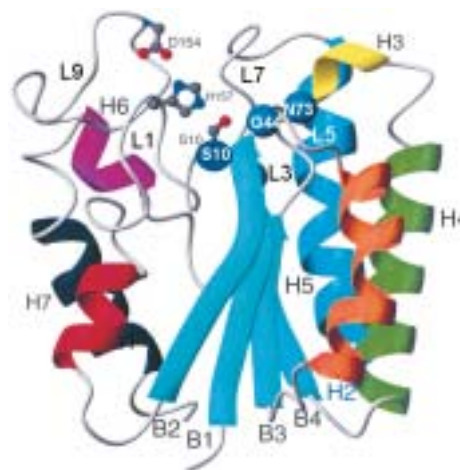


Fig. 1. Ribbon representation of the X-ray crystal structure of TEP-I. The secondary structures are deduced from NMR restraints and chemical shift indices (Lin, et al., 1998). The designations of the helices and strands are given next to the respective elements. The catalytic triad, Ser¹⁰, Asp¹⁵⁴ and His¹⁵⁷, are shown in the stick-and-ball rendering and the blue balls represent the putative oxyanion holes, Gly⁹, Ser⁴³ and Asn⁷³. This figure was prepared using the program MOLMOL.⁴⁴

($= 1/T_1$), $^{15}\text{N-R}_2$ ($= 1/T_2$), and heteronuclear ^1H - ^{15}N -NOE (XNOE), were obtained at both 11.74 T (500.13 MHz for proton operating frequency) and 14.09 T (600.13 MHz). A total of 135 (128) resonances at 14.09 T (Numbers in parentheses were measured at 11.74 T) were determined (Fig. 2). These data were analyzed with Modelfree formalism. In this approach, the molecular overall and internal motions are assumed to be independent. This assumption is rigorously valid for the case of isotropic molecular overall motion and is approximately accurate for anisotropic molecular overall motion.^{29,30} Model-free formalism uses the magnitude of order parameters to describe the degree of angular restriction of the motion of the NH bond vector. The motional time scales are expressed as effective correlation times or conformational exchange rates. Thus, a mobile region displaying large amplitude angular fluctuations on the ps/ns time scale has a lower

value of the order parameter, whereas a rigid region should have a higher value of the order parameter. The residue-specific model-free dynamic parameters are the generalized order parameters (S^2), the effective correlation times for internal motions (τ_e), and the conformational exchange terms (R_{ex}).

The spatial distributions, in sausage representations, of S^2 and R_{ex} , extracted from Fig. 2 are shown in Fig. 3. Residues Ser¹⁰, Asp¹⁵⁴ and His¹⁵⁷, comprising the catalytic triad, are shown in the stick-and-ball rendering. The three blue balls correspond to the three putative oxyanion holes (Asp⁹, Ser⁴³ and Asn⁷³). As expected, rigid residues are located mostly in the core region formed by the β -sheet and the helices. The most mobile residues are located mostly in the loop regions, particularly those forming the active site. Of particular interest is the presence of several slowly exchanging residues near the active site. The three putative oxyanion hole residues are all located next to residues that display slow exchange, although the three oxyanion-hole residues are quite rigid themselves, as judged from their large order parameters. In summary, TEP-I is an enzyme with a flexible active site supported by a rigid framework. Slow fluctuation of the binding site geometry is predicted based on the present dynamics results. The functional significance and its relationship to catalytic activity are yet to be further defined.

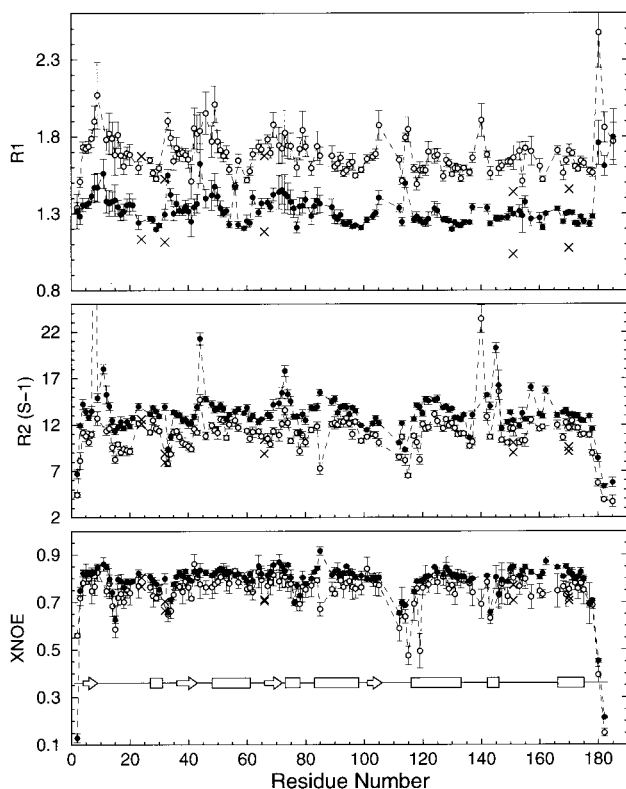


Fig. 2. The relaxation parameters of TEP-I measured at 310 K, and at both 11.74 T (open circles) and 14.09 T (filled circles). R_1 (top), R_2 (middle), and XNOE (bottom) are plotted as a function of residue number. The locations of the secondary structure elements are also shown. Arrows represent β -strands and bars represent α -helices. Symbols of X represent the relaxation parameters for tryptophan indole N¹.

Hydrogen bond network involving catalytic triad residues²¹

Many enzymes use the Ser-His-Asp catalytic triad for enhancing catalytic activities. What are the properties that allow this apparatus to work is a question central to the understanding of the catalytic mechanism of these serine enzymes. A great deal of attention has been devoted to the understanding of the catalytic triad for the past more than thirty years.^{31,32} Several theories have been proposed to explain how the triad works, including the charge-relay model,^{33,34} "low barrier" hydrogen bond (LBHB)" theory,³⁵⁻³⁷ and the "imidazole ring flip".³⁷ In order to understand the catalytic mechanism it is essential to understand the hydrogen-bonding network of the catalytic triad.

Shown in Fig. 4 are low-field ^1H NMR spectra of various protein samples. Spectra were obtained at 2 °C in 50 mM phosphate buffer, pH 6.1. Under the experimental conditions two resonances at 15.4 ppm and 14.3 ppm for the wild-type protein were observed. In the free enzyme these two resonances can be observed only at low temperatures in H_2O , and thus are due to exchangeable protons. These extremely low-field resonances have been observed in several serine pro-

teases.^{36,38,39} Resonances at 15 ppm or lower field have been assigned to the N ¹H of the catalytic His residues. The detection of this low-field resonance provided strong evidence

supporting the formation of a strong hydrogen bond between His-N ¹H and the carboxyl oxygen of the catalytic Asp. Following this argument we can tentatively assign this reso-

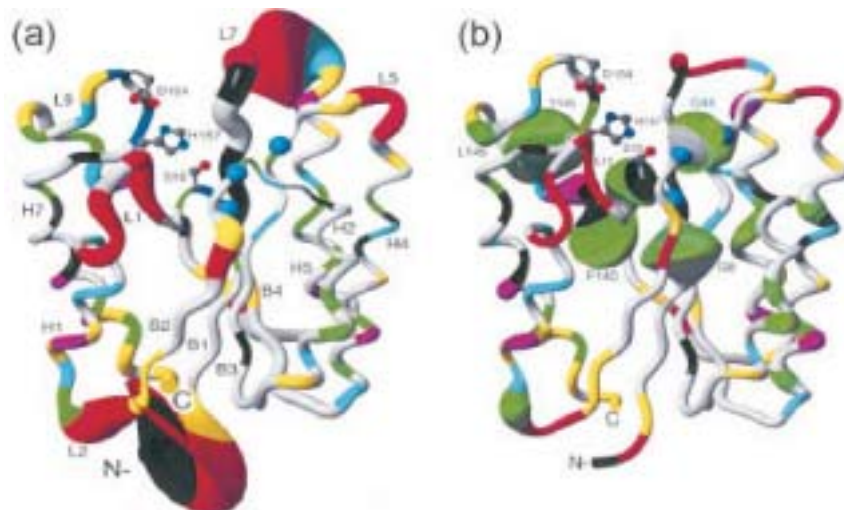


Fig. 3. Sausage representations of the spatial variations of dynamic parameters. (a) The diameter of the sausage is inversely related to the order parameter of the ¹⁵N-¹H vector of the given residue. (b) The diameter of the sausage is directly related to the exchange rates, R_{ex} . The colors are coded according to models employed to fit the relaxation data for each residue as follows: gray, model 1; orange, model 2; green, model 3; magenta, model 4; and red, model 5. Overlapping residues are colored cyan. Missing residues are colored black. This figure was prepared using the program MOLMOL.⁴⁴

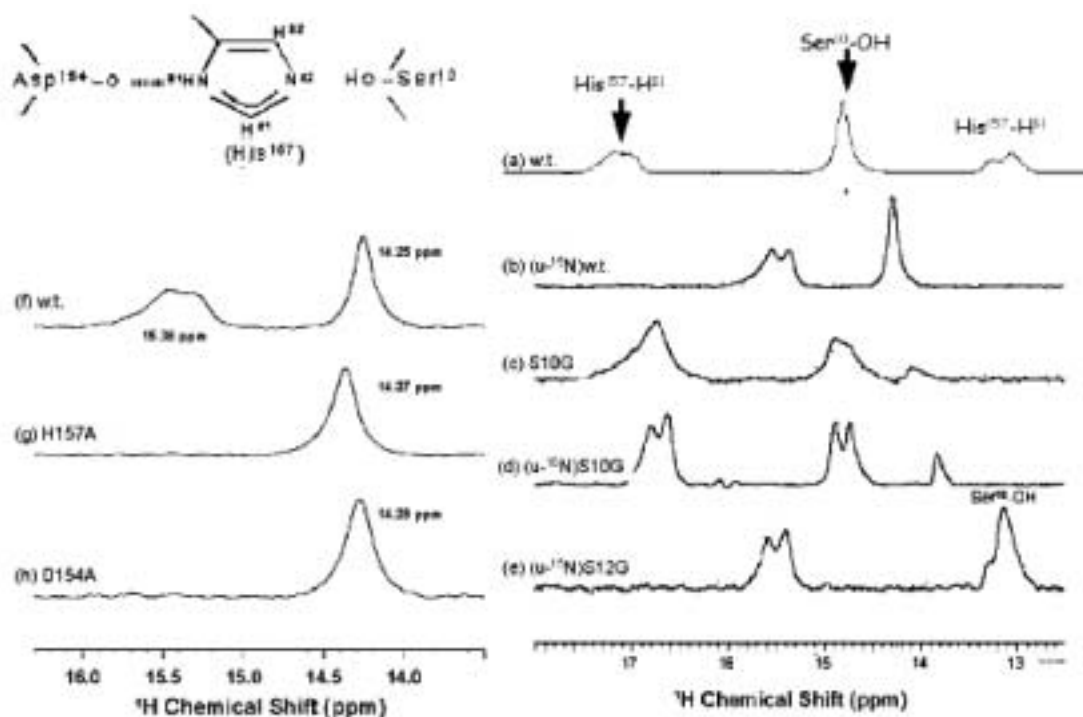


Fig. 4. ¹H NMR spectra of various TEP-I mutant samples (0.5–2.2 mM) in 50 mM phosphate buffer, pH 6.1, 10% D₂O. NMR spectra were obtained at 2 °C with 1331 pulse sequence with carrier frequency set at 4.7 ppm using a Bruker AMX500 spectrometer.

nance to His¹⁵⁷-N¹H. This assignment is supported by the splitting of this resonance into a doublet of $^1J_{\text{NH}} = 90$ Hz in the spectrum obtained with (u-¹⁵N)TEP-I (Fig. 4b)⁴⁰ and the disappearance of this resonance in the spectra of H157A and D154A mutants (Fig. 4g and h). The absence of splitting of the 14.3 ppm resonance into a doublet in the spectrum obtained with the (u-¹⁵N)TEP-I sample suggests that it is not a nitrogen proton. To further assign this resonance we have prepared two mutants, the S10G mutant and the S12G mutant. The large upfield shift of the 14.3 ppm resonance to 13.2 ppm in S12G suggests that the 14.3 ppm resonance is from a proton near Ser¹² residues. Thus, we tentatively assign the 14.3 ppm resonance to Ser¹⁰-O H.

The assignment of these two low field resonances allowed us to determine the pK_a of His¹⁵⁷ and Ser¹⁰ from pH-induced chemical shift changes. The pK_a of His¹⁵⁷ deduced from the titration curve of N¹H is ~ 6.8. The near invariance of the Ser¹⁰-O H resonance with the titration of the His¹⁵⁷-N² nitrogen suggests that the Ser¹⁰-O H is not hydrogen bonded to His¹⁵⁷-N². In the X-ray crystal structure Ser¹⁰-O was found to be 3.6 Å from His¹⁵⁷-N², too far to form a hydrogen bond, in agreement with our results. Interestingly, we found that Ser¹⁰-O is 2.58 Å from the backbone carbonyl group of Ile⁴², well within the distance for forming a hydrogen bond. Thus, we propose that in free enzyme Ser¹⁰-O H is hydrogen bonded to the carbonyl group of Ile⁴², causing it to resonate at low field.

Structure of the michaelis complex²²

Fig. 5 depicts the mechanism of inhibition of TEP-I by the transition state analogue compound, diethyl-p-nitrophenyl phosphate (DENP).^{41,42} Following the formation of Michaelis complex the mechanism-based inhibitor DENP forms a covalent tetrahedral complex with the active site Ser¹⁰. The structure of the free enzyme and the transition state complex with DENP are available, but the structure of the Michaelis complex is hard to determine. Ligand binding to enzymes can be followed by various techniques, including affinity capillary electrophoresis.⁴³ We have employed the NMR method to characterize the structural transition of TEP-I upon DENP binding. The addition of DENP resulted in the appearance of new resonances with a concomitant decrease in intensities corresponding to free enzyme. We observed two sets of new resonances: (1) Transient resonances that appear only for a short period of time after the addition of DENP and disappear again after prolonged exposure to the inhibitor; and (2) Resonances that appear at a later time. At a proper DENP molar ratio and by adjusting pH and temperature conditions it is pos-

sible to obtain spectra containing only the intermediate species and the final complex, only the intermediate, or only the final complex. In general, formation of the intermediate species is fast, but the conversion from the intermediate species to the final complex is slow. Fig. 6 shows the superposition of a portion of ¹⁵N-HSQC spectra of a free enzyme (blue) and a sample containing only the Michaelis complex (red) (Fig. 6a). Fig. 6b shows the corresponding spectra of Michaelis complex (blue) and the tetrahedral complex (red). Fig. 6c shows the composite amide ¹H and ¹⁵N chemical shift differences between free enzyme and the Michaelis complex and between Michaelis complex and the tetrahedral complex (Fig. 6d). In both steps the residues involved appear to be localized in similar four loop segments: Loop L1 region (Asp⁹-Gly¹⁴) which contains the catalytic Ser¹⁰; Loop L3 region (Ala⁴⁰-Thr⁴⁶); Loop L5 region (Leu⁷⁰-Leu⁷⁶); and Loop L9 region (Phe¹⁴⁰-His¹⁵⁷) which contains two catalytic residues Asp¹⁵⁴ and His¹⁵⁷. Together with loop L7 and helix H3 these

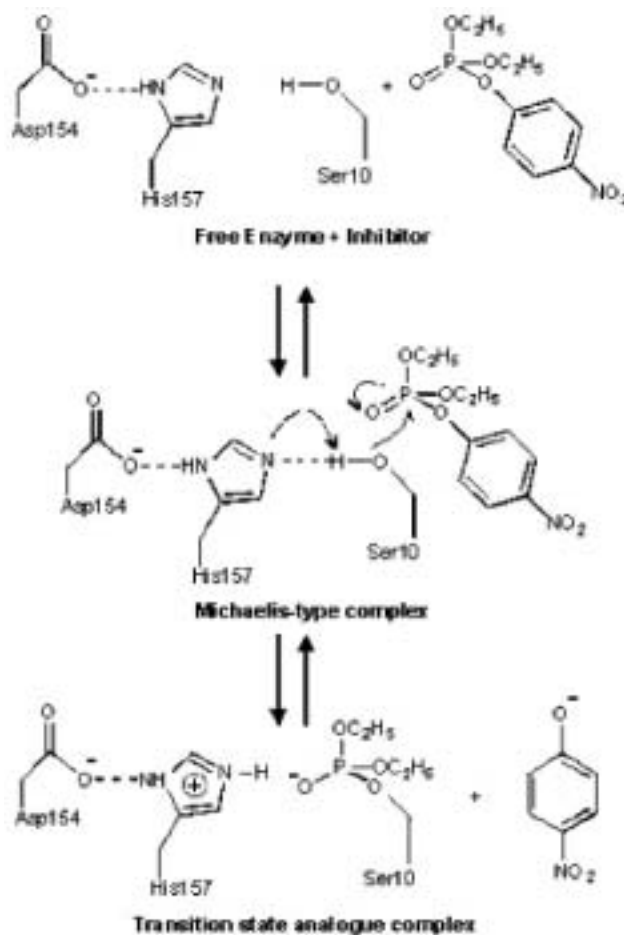


Fig. 5. Proposed mechanism of the inhibition of DENP on the catalysis of TEP-I.

segments make up the active site.²⁰ All the catalytic triad residues (Ser¹⁰, Asp¹⁵⁴ and His¹⁵⁷) are perturbed, confirming that indeed DENP binds to the active site in a functionally relevant manner. Closer inspection of the details of the structural transitions reveals several interesting points: (1) Residues exhibiting the largest shifts, namely those located in loops L1 and L3, cluster around Ser¹⁰ while the residues around Asp¹⁵⁴ show much less shift perturbation. Thus, DENP binds to a site near the Ser¹⁰-OH group, as expected. (2) In free enzyme the amide resonance of Ser¹⁰ cannot be detected, probably due to line broadening caused by conformational exchange.²⁰ However, in MC a new resonance was observed in the ¹⁵N-HSQC spectrum of (u-¹⁵N-Ser)TEP-I/DENP sample and this resonance was assigned to Ser¹⁰, since this is the only unassigned serine residue. Our ability to detect this resonance in the MC and tetrahedral complex states suggests that binding of

DENP stabilizes the conformation of Ser¹⁰, or that binding causes the water exclusion from the binding pocket to reduce the line broadening of the Ser¹⁰ amide proton. (3) Transition from the MC to the tetrahedral complex was characterized by additional shifts in several resonances. The most prominent of which are Ser¹⁰, Gly⁴⁴, and Ala¹¹¹. The large chemical shift change observed for Ser¹⁰ and Gly⁴⁴ in the second step suggests the possibility of hydrogen bond formation between the phosphate group of DENP and ¹H^N of these groups, supporting the speculation that these two groups might serve as the proton donors to the oxyanion. Thus the present work represents the first direct experimental determination of the hydrogen bond formation between the phosphate group of the transition state inhibitor and the oxyanion-hole groups in solution. The observation of large chemical shifts in residues Ala¹¹¹ and Ala¹²⁰ from loop 7, the most flexible loop in TEP-

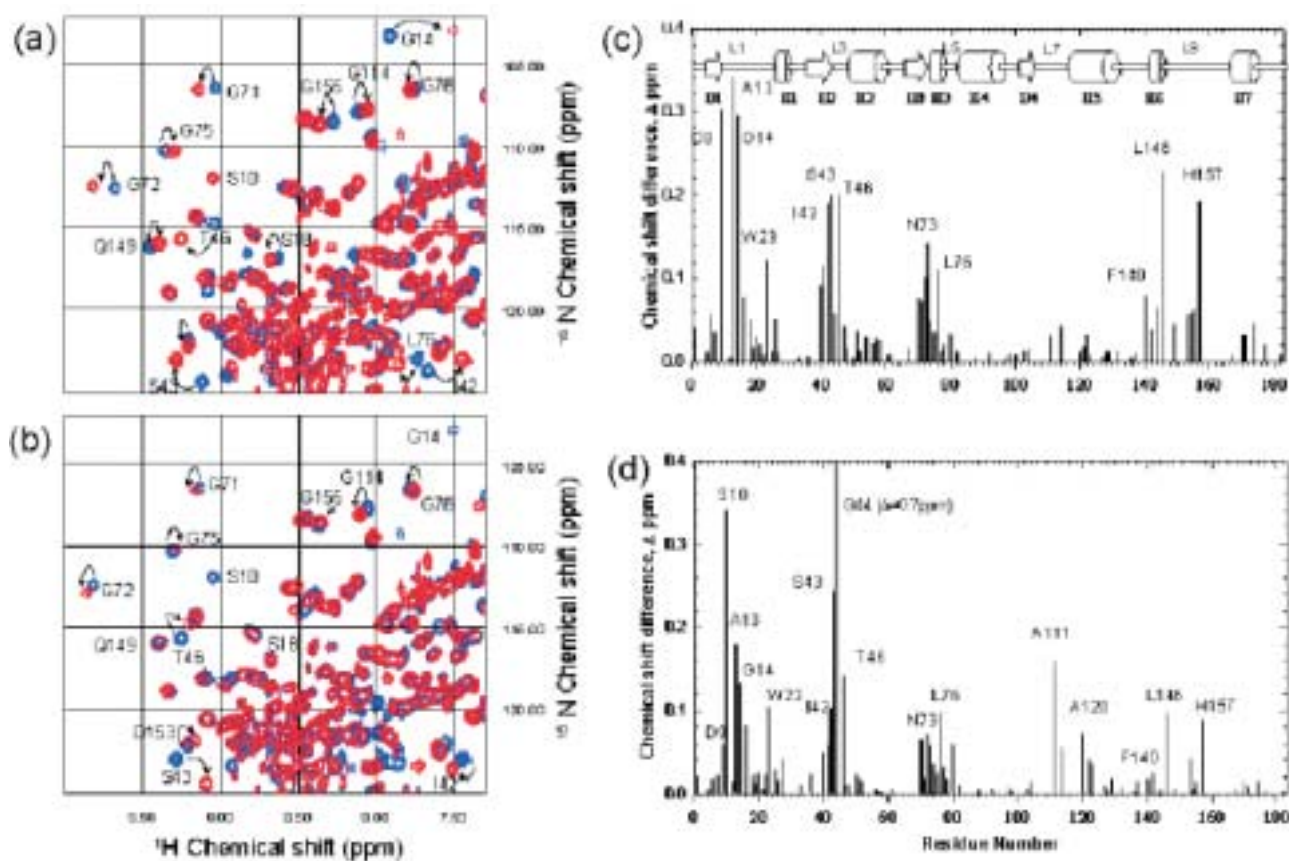


Fig. 6. (a) Superposition of a portion of ¹⁵N-HSQC spectra of a free enzyme (blue) and a sample containing only the Michaelis complex (red). The sample which contains only Michaelis complex was obtained by incubating TEP-I with 10 time excess of DENP at room temperature for 5 min. (b) Superposition of a portion of ¹⁵N-HSQC spectra of Michaelis complex (blue) and the tetrahedral complex (red). The sample which contains only the tetrahedral complex was obtained by equilibrating the sample in (c) at 310K for over 10 hours. (c) Chemical shift differences between free enzyme and the Michaelis complex. (d) Between the Michaelis complex and the tetrahedral complex. The sequence locations of the secondary elements are shown in the top figure.

I,²⁰ might indicate a large-scale movement of this loop at the second step.

Based on present results we propose the following structural events taking place following DENP binding. In the Michaelis complex DENP binds to the active site with the phosphate group already positioned near Ser¹⁰, thus causing large chemical shift perturbations of the surrounding amide protons. Binding of DENP stabilizes the floppy Ser¹⁰ residue to adapt a defined conformation. Our previous studies showed that the hydrogen bond between Asp¹⁵⁴-O and His¹⁵⁷-H¹ was also perturbed at this step, as shown by the disappearance of the low field proton resonance assigned to the His¹⁵⁷-H¹.²¹ Perturbation of ¹H^N resonances of Leu¹⁴⁶ and His¹⁵⁷ indicates structural changes in loop 9 at this step. Thus, residues perturbed at this step were confined mainly to the conserved segments comprising the binding pocket (L1, L3, H3, L5 and L9).

The second step of conversion from Michaelis complex to the tetrahedral complex involves the covalent binding of the phosphate group to Ser¹⁰-OH. Residues affected at this step are located mostly in the same four conserved segments, suggesting a continuous adjustment of the active site geometry. A prominent feature of the structural changes at this step is the possible formation of hydrogen bonds between the phosphate group of DENP and the amide protons of the Ser¹⁰ and Gly⁴⁴, as evident from the large chemical shift changes for these two amide protons. Thus, Ser¹⁰-H^N and Gly⁴⁴-H^N serve as oxyanion hole proton donors to stabilize the tetrahedral complex. The ¹H^N resonance of Asn⁷³ was perturbed substantially at the first step, although not as large as that observed for Ser¹⁰ and Gly⁴⁴, probably because the phosphate group does not bind directly to the amide proton of Asn⁷³. Conversion of MC to the tetrahedral complex is further accompanied by the structure changes of the floppy loop L7 region, reflecting a possible further tightening up of the binding pocket. Thus, the prominent feature of the structural changes induced by DENP binding is the sequential structural rearrangement involving the four conserved segments.

Future perspectives

The molecular basis of enzyme catalysis is far from understood. NMR is the most promising method in probing this important biochemical phenomenon. TEP-I is an idea model system for studying enzyme catalysis. We have made significant progress toward understanding the catalytic mechanism of TEP-I. Questions that are still outstanding include the detailed molecular steps, the kinetics and energetics of various intermediate species in the catalytic process, and the role of

molecular dynamics in catalysis. Work for addressing these questions are in progress. The establishment of the High-Field Biomacromolecular NMR Core Facility of the National Program for Genomic Medicine, with the installation of ultra-high field NMR spectrometer at 800 MHz and the cryoprobes will greatly enhance our ability in this regard. For this, we owe much to the vision and strong support of Prof. Sunney I. Chan.

ACKNOWLEDGEMENTS

This work was supported in part by Academia Sinica and by a grant (92-2113-M-001-056) (THH) from the National Science Council of The Republic of China. The NMR spectra and the ESI-MS data were obtained, respectively, at the High-field Biomacromolecular NMR Core Facility and at the Core Facility for Proteomic Research, National Program for Genomic Medicine, The Republic of China.

Received March 23, 2004.

REFERENCES

1. Kraut, J. *Science* **1988**, 242, 533.
2. Eyring, H. *Chem. Rev.* **1935**, 17, 65.
3. Pauline, L. *Chem. Eng. News* **1946**, 24, 1375.
4. Kurz, J. L. *J. Am. Chem. Soc.* **1963**, 85, 987.
5. Schramm, V. L. *Annu. Rev. Biochem.* **1998**, 67, 693.
6. Hammes, G. G. *Protein Sci* **1998**, 7, 799.
7. Chang, G. G. *J. Chin. Chem. Soc.* **1992**, 39, 711.
8. Wolfenden, R. *Nature* **1969**, 223, 704.
9. Lolis, E.; Petsko, G. *Ann. Rev. Biochem.* **1990**, 59, 597.
10. Pacaud, M.; Uriel, J. *Eur. J Biochem.* **1971**, 23, 435.
11. Cho, H.; Cronan, J. E. Jr. *J. Biol. Chem.* **1993**, 268, 9238.
12. Ichihara, S.; Matsubara, Y.; Kato, C.; Akasaka, K.; Mizushima, S. *J. Bacteriol.* **1993**, 175, 1032.
13. Lee, Y. L.; Chen, J. C.; Shaw, J. F. *Biochem. Biophys. Res. Commun.* **1997**, 231, 452.
14. Upton, C.; Buckley, J. T. *Trends Biochem. Sci.* **1995**, 20, 178.
15. Spencer, A. K.; Greenspan, A. D.; Cronan, J. E. Jr. *J. Biol. Chem.* **1978**, 253, 5922.
16. Barnes, E. M. Jr.; Wakil, S. J. *J. Biol. Chem.* **1968**, 243, 2955.
17. Cho, H.; Cronan, J. E. Jr. *J. Bacteriol.* **1994**, 176, 1793.
18. Cho, H.; Cronan, J. E. Jr. *J. Biol. Chem.* **1995**, 270, 4216.
19. Lin, T. H.; Chen, C. P.; Huang, R. F.; Lee, Y. L.; Shaw, J. F.; Huang, T. H. *J. Biomol. NMR* **1998**, 11, 363.

20. Huang, Y. T.; Liaw, Y. C.; Gorbatyuk, V. Y.; Huang, T.-H. *J. Mol. Biol.* **2001**, 307, 1075.
21. Tyukhtenko, S. I.; Litvinchuk, A. V.; Chang, C. F.; Leu, R. J.; Shaw, J. F.; Huang, T.-H. *FEBS Lett.* **2002**, 528, 203.
22. Tyukhtenko, S. I.; Litvinchuk, A. V.; Chang, C.-F.; Shaw, J.-F.; Liaw, Y. C.; Huang, T.-H. *Biochemistry* **2003**, 42, 8289.
23. Dalgarno, D. C.; Levine, B. A.; Williams, R. J. P. *Biosci. Rep.* **1983**, 3, 443.
24. Spera, S.; Bax, A. *J. Am. Chem. Soc.* **1991**, 113, 5490.
25. Wishart, D. S.; Sykes, B. D. *Methods Enzymol.* **1994**, 239, 363.
26. Wuthrich, K. In *NMR of Proteins and Nucleic Acids*; Wiley Interscience: New York, 1986.
27. Liaw, Y. C. (personnal communication).
28. Molgaard, A.; Kauppinen, S.; Larsen, S. *Structure Fold Des.* **2000**, 8, 373.
29. Lipari, G.; Szabo, A. *J. Am. Chem. Soc.* **1982**, 104, 4546.
30. Lipari, G.; Szabo, A. *J. Am. Chem. Soc.* **1982**, 104, 4559.
31. Bachovchin, W. W. *Magn. Reson. Chem.* **2001**, 39, S199.
32. Frey, P. A. *Magn. Reson. Chem.* **2001**, 39, S190.
33. Blow, D. M.; Birktoft, J. J.; Harley, B. S. *Nature* **1969**, 221, 337.
34. Hunkapiller, M. W.; Smallcombe, S. H.; Whitaker, D. R.; Richards, J. H. *J. Biol. Chem.* **1973**, 248, 8306.
35. Cassidy, C. S.; Lin, J.; Frey, P. A. *Biochem. Biophys. Res. Commun.* **2000**, 273, 789.
36. Mildvan, A. S.; Harris, T. K.; Abeygunawardana, C. *Methods Enzymol.* **1999**, 308, 219.
37. Ash, E. L.; Sudmeier, J. L.; Day, R. M.; Vincent, M.; Torchilin, E. V.; Haddad, K. C.; Bradshaw, E. M.; Sanford, D. G.; Bachovchin, W. W. *PNAS* **2000**, 97, 10371.
38. Robillard, G.; Shulman, R. G. *J. Mol. Biol.* **1972**, 71, 507.
39. Steitz, T. A.; Shulman, R. G. *Ann. Rev. Biophys. Bioeng.* **1982**, 11, 419.
40. Bachovchin, W. W. *Proc. Natl. Acad. Sci.* **1985**, 82, 7948.
41. Millard, C.; Koellner, G.; Ordentlich, A.; Shafferman, A.; Silman, I.; Sussman, J. *J. Am. Chem. Soc.* **1999**, 121, 9883.
42. Massiah, M. A.; Viragh, C.; Reddy, P. M.; Kovach, I. M.; Johnson, J.; Rosenberry, T. L.; Mildvan, A. S. *Biochemistry* **2001**, 40, 5682.
43. Chu, Y. H.; Zhang, X.; Tu, J. *J. Chin. Chem. Soc.* **1998**, 45, 713.
44. Koradi, R.; Billeter, M.; Wuthrich, K. *J. Mol. Graphics* **1996**, 14, 51.